CODEN IEJMAT *Internet Electronic Journal of Molecular Design* **2008**, *7*, 12–29 ISSN 1538–6414
BioChem Press http://www.biochempress.com

Inter*net* Electronic Journal of Molecular Design

January 2008, Volume 7, Number 1, Pages 12–29

Editor: Ovidiu Ivanciuc

Comparative Modeling and Docking Studies of *Mycobacterium tuberculosis* H_{37}RV rpoB Protein

P. Nataraj Sekhar,[1] P. B. Kavi Kishor,[1] V. C. K. Reddy,[2] E. Prem Kumar,[1] A. Anitha,[1] Ranjith Kumar M.,[1] and L. Ananda Reddy [1]

[1] Department of Genetics, Osmania University, Hyderabad–500 007, India
[2] Osmania Medical College, Hyderabad–160 016, India

Received: November 21, 2006; Revised: December 15, 2007; Accepted: January 5, 2008; Published: January 31, 2008

Citation of the article:
P. N. Sekhar, P. B. K. Kishor, V. C. K. Reddy, E. P. Kumar, A. Anitha, R. Kumar M., and L. A. Reddy, Comparative Modeling and Docking Studies of *Mycobacterium tuberculosis* H_{37}RV rpoB Protein, *Internet Electron. J. Mol. Des.* **2008**, *7*, 12–29, http://www.biochempress.com.

Copyright © 2008 BioChem Press

Inter*net* **Electronic** Journal of Molecular Design

BioChem Press
http://www.biochempress.com

Comparative Modeling and Docking Studies of *Mycobacterium tuberculosis* $H_{37}RV$ rpoB Protein

P. Nataraj Sekhar,[1] P. B. Kavi Kishor,[1] V. C. K. Reddy,[2] E. Prem Kumar,[1] A. Anitha,[1] Ranjith Kumar M.,[1] and L. Ananda Reddy [1,*]

[1] Department of Genetics, Osmania University, Hyderabad–500 007, India
[2] Osmania Medical College, Hyderabad–160 016, India

Received: November 21, 2006; Revised: December 15, 2007; Accepted: January 5, 2008; Published: January 31, 2008

Internet Electron. J. Mol. Des. **2008**, *7* (1), 12–29

Abstract

Motivation. Recently the entire *rpoB* genes of *Mycobacterium leprae* and *M. tuberculosis* have been sequenced and several mutations associated with rifampin resistance have been identified in both species. Since no crystal structure was available for the rpoB protein, a three–dimensional (3D) structure of rpoB protein (a protein complex involved in the polymerization of ribonucleotides) was generated computationally in order to understand the mechanisms of ligand binding and the interactions between the ligand and the protein. Docking experiments for rpoB were performed with its inhibitors to better understand the drug interactions and rifampin resistance, thus allowing us to predict the mutations with respect to the active site of the enzyme and its inhibitor and binding domain. This study may thus help in the development of rapid diagnostic tests for tuberculosis.

Method. A three–dimensional model of the rpoB protein (NP_215181) is generated based on the crystal structure of the *Thermus thermophilus* (PDB: 2CW0) by using the software MODELLER6v2. The structure having the lowest score was used as starting point for further minimization computations. The structure having the lowest energy generated by the conjugate gradient energy minimization, with less than 0.05 kcal/mol energy gradient, was further assessed by PROCHECK, which showed that the refined model is reliable. In order to understand the mechanisms of ligand binding and the interaction between the ligand and the rpoB protein complex, a flexible docking study was performed using GOLD software.

Results. Docking results indicated that the fourth binding pocket falls in the active site of the protein. They also indicated that ciprofloxacin is the more preferred inhibitor and that the residues Gln429, Arg448, Ser450 are determinant residues in binding as they have strong hydrogen bonding contacts with the ligand. Thus, this study is useful for the synthesis of novel rpoB inhibitors. Based on docking studies, the bioactive conformations of the ligands obtained will be useful in building structure–based 3–D QSAR models.

Conclusions. Our results indicate that ciproflaxin is the best inhibitor against rifampicin resistant rpoB protein.

Keywords. Homology modeling; docking; GOLD; *Mycobacterium leprae*; *Mycobacterium tuberculosis* H37RV; *Thermus thermophilus*.

Abbreviations and notations

BLAST, basic local alignment search tool	PDB, protein databank
GOLD, genetic optimization for ligand docking	RMS, root mean–square
NCBI, national center for biotechnology information	SCRs, structurally conserved regions
pdfs, probability density functions	SVRs, structurally variable regions

* Correspondence author; E–mail: lakkireddy_anandareddy@rediffmail.com.

1 INTRODUCTION

Tuberculosis (TB), though curable, still remains a major killer disease worldwide. It was estimated that the magnitude of the problem has increased to 10–12 million cases from 2000 to 2005 [1]. Nearly 32% of the world population and 30% of the population in India have been affected with *Mycobacterium tuberculosis* worldwide. 80% new TB cases were found every year in 22 countries, with more than half the cases occurring in five Southeast Asian countries [2]. The problem of tuberculosis has increased with the emergence of multidrug resistant (MDR) strains of *M. tuberculosis*. The genus *Mycobacterium* comprises a wide range of organisms, including obligate parasites causing serious human and animal diseases. Human infections are caused by slowly growing mycobacteria that need more than a week to form visible colonies.

Traditionally, the definitive diagnosis of mycobacterial infections was dependent on the isolation and identification of causative agents and requires specific physiological and biochemical tests. The procedures for these tests are complex, laborious and usually impeded by the slow growth of mycobacteria in clinical laboratories. In particular, *Mycobacterium leprae* has not been cultivated *in vitro*. There are an increasing number of reports of infections caused by mycobacteria other than *M. tuberculosis* (MOTT), especially in association with human immunodeficiency virus infection. These are rarely disease associated, not known previously or newly recognized mycobacteria that are not easy to identify. Also, due to their phenotypic similarity to certain species, they cannot be easily characterized by the conventional methods of identification. The systematics of mycobacteria may help in the identification of these phenotypically similar mycobacterial species.

Recently, the *rpoB* gene was used as an alternative tool to identify mycobacteria [3]. The gene *rpoB* encodes the β–subunit of RNA polymerase. The *rpoB* nucleotide sequences of three mycobacterial species were previously known [4–6]. It is known that missense mutations within *rpoB*'s limited region are related to the resistance of rifampin in *M. tuberculosis* [7]. Rifampin is a key component of multidrug therapies not only for tuberculosis but also for leprosy and it is recommended for the treatment of leprosy [8,9]. Due to the widespread usage of rifampin, rifampin–resistant bacterial stains have emerged [10–15]. Hence, there is a need to identify rifampin susceptible and resistant strains [16]. The drug target in *E. coli* appears to be the β–subunit of DNA–dependent RNA polymerase, which is encoded by the *rpoB* gene [17,18]. Comparative studies of several protein sequences of *rpoB* showed six highly conserved regions (regions I to VI) [19] with homology in the large subunits of RNA polymerases of eukaryotic origin [20–23]. It appears from the studies that rifampin resistance is due to missense mutations within these conserved regions [24–27]. Besides, majority of these mutations are tightly clustered in a short region, cluster I of region II, near the middle of *rpoB* [24]. Sequence analysis of *M. leprae rpoB*

gene showed extensive homology to the other prokaryotic genes and proteins [28]. The structures of those sites identified on the basis of their interactions with rifampin in fact were well conserved. The aim of the present study is to develop three–dimensional structure of rifampin resistant rpoB protein from *Mycobacterium tuberculosis* and to see the drug interactions for better understanding of the resistance mechanism that can lead to the development of rapid diagnostic test.

2 MATERIALS AND METHODS

2.1 3D Model Building

To predict the three–dimensional structure for the amino acid sequence of *M. tuberculosis* [Accession Number: NP_215181] obtained from the NCBI database, the query sequence was searched against PDB (Protein Databank) [29,30] to find out the protein structures of the related family to be used as a template by the BLAST program using BLOSUM62 scoring matrix with a word size of 3 amino acids. Sequence that showed maximum identity with high score and less e–value were aligned, and used as a reference structure to build a 3D model for rpoB. The 3D–models of rpoB from *M. tuberculosis* were generated using the automated homology modeling software MODELLER6v2 [31] on IRIX operating environment using Silicon Graphics Octane O_2 stations (Silicon Graphics Inc., Mountain View, CA). The method is based on comparative protein structure modeling optimally satisfying spatial restraints, expressed as probability density functions (pdfs) for the location of each atom in the protein. The 3D model of a protein is obtained by optimizing the molecular pdf such that the model violates the input restraints as little as possible. The optimization procedure is a variable target function method that applies the conjugate gradients algorithm to positions of all non–hydrogen atoms. The coordinates for the structurally conserved regions (SCRs) for rpoB were assigned from the template using pairwise sequence alignment, based on the Needleman–Wunsch algorithm [32,33]. The program also includes *ab initio* structure prediction for modeling of highly variable regions termed such as loop regions which are difficult to predict by homology modeling.

2.2 Minimization Method

The structure having the least MODELLER objective function was improved by energy minimization. Initial geometric optimizations were carried out using the standard Tripos force field with delta energy change 0.05 kcal/mol energy convergence criteria and a distant dependent dielectric constant of 4.0 R to take into account the dielectric shielding in proteins, and with Gasteiger–Marsili charges and a non–bonding interaction cut–off of 15 Å. All hydrogen atoms were included during the calculation. After 100 steps of Powell minimization, a conjugate gradient energy minimization of the full protein was carried out until the root mean–square (r.m.s) gradient

was lower than 0.05 kcal/mole/Å. The default parameters used for minimization are max displacement 0.01 Å; simplex threshold 1000; LS accuracy 0.001; LS step–size 0.001; nonbonded reset 10Å; RMS displacement 0.001 Å; gradient 0.05 Å; simplex iterations 100; derivative rest 100 iterations; color option–force.

2.3 Molecular Modeling Software

All calculations were performed using the SYBYL software suite implemented on a Silicon Graphics Octane O2 workstation, operating under IRIX (SYBYL 6.7, Tripos Inc., 1699, South Hanley Rd., St. Louis, Missouri, 63144, USA). Structural diagrams were prepared using OPEN EYE (Open Eye Scientific Software, Santa Fe, NM) and SPDBV software [34].

2.4 Model Validation

The lowest MODELLER energy structure obtained from MODELLER6v2 was used to assess the degree of violation of the template–derived restraints by Ramachandran's map using PROCHECK, a program used to check the stereo chemical quality of protein structures [35]. Quality evaluation of the model for the environment profile was also predicted using ERRAT (structure evaluation server) [36]. The final refined model was evaluated for its atomic contacts using the Whatif program to identify bad packing of side chain atoms or unusual residue contacts [37]. This model was used to identify the active site and for docking the inhibitors with the enzyme. Color figures were generated using SYBYL and OPENEYE software program.

2.5 Active Site Identification for the rpoB Enzyme

The active site of the energy–minimized structure of rpoB from *M. tuberculosis* was identified using SiteID based on grid method of SYBYL software suite (Figure 4). This method generated many possible spheres of the radius of water inside the protein molecules in search of the largest space or cluster available, which could be identified as active site. A flood fill algorithm, similar to one implemented in CAVITY was used [38]. For each solvent molecule in the pocket, all atoms in the protein lying within a specific distance of 5 Å are considered. The unions of all such atoms are considered as belonging to the active site. In addition to this, electrostatic or polar surface identification method was used to distinguish between the actual site and the other smaller cluster of sites. The default parameters used in grid method are grid resolution 1.0 Å, protein film depth 3.0 Å, atomic film depth 3.0 Å, exclusion radius 2.5 Å, inclusion radius 8.0 Å, minimum population of protein atoms within inclusion radius 80, inclusion radius (grids only) 2.0, minimum population of grid points within inclusion radius 6, cluster inclusion radius 3.0 Å, minimum population of grid points in a cluster 10 and maximum population of grid points in a cluster 300.

2.6 Docking Studies

The ligands, including all hydrogen atoms, were built and minimized with the SYBYL software suite as described above. Genetic optimization for ligand docking (GOLD) version 2.1.2 (Cambridge Crystallographic Data Center, Cambridge, United Kingdom) was used for docking rpoB protein for 50 times [39]. This method allows a partial flexibility of protein and full flexibility of ligand. All water molecules and heteroatoms were removed from the protein to evaluate the scoring function in GOLD software. For each of the 50 independent GA runs, a maximum number of 100000 GA operations were performed on a set of five groups with a population size of 100 individuals. Default cutoff values of 2.5 Å (dH–X) for hydrogen bonds and 4.0 Å for van der Waals distance were employed. The RMSD values for the docking calculations are based on the RMSD matrix of the ranked solutions. The active site was defined as the collection of protein residues enclosed within a 15 Å radius sphere of the site 4 predicted using SITEID module of SYBYL. The annealing parameters for van der Walls and hydrogen bonding were set to 4.0 Å and 2.5 Å respectively. The parameters used for genetic algorithm were population size (100), selection pressure (1.1), number of operations (1,00,000), number of islands (5), niche size (2), migrate (10), mutate (95) and crossover (95). The default speed selection was used to avoid a potential reduction in docking accuracy. Fifty genetic algorithm runs with default parameter settings were performed without early termination. To estimate the protein–ligand complexes, the scoring function, GOLD score was employed which is based on the following four components: (1) protein–ligand hydrogen bond energy (external H–bond); (2) protein–ligand van der Waals energy (external vdw); (3) ligand internal van der Waals energy (internal vdw); (4) ligand intramolecular hydrogen bond energy (internal– H– bond). The external van der Walls score is multiplied by a factor of 1.375 when the total fitness score is computed. This is an empirical correction to encourage protein–ligand hydrophobic contact. The fitness function has been optimized for the prediction of ligand binding positions. Gold Score = S (hb_ext) + S (vdw_ext) + S (hb_int) + S (vdw_int), where S (hb_ext) is the protein–ligand hydrogen bond score, S (vdw_ext) is the protein–ligand van der Waals score, S (hb_int) is the score from intramolecular hydrogen bond in the ligand and S (vdw_int) is the score from intramolecular strain in the ligand [39]. The protein–ligand complex is generated using the GOLD package without constraints between the ligand and the specific amino acids of the pocket. The algorithm exhaustively searches the entire rotational and translational space of the ligand with respect to the receptors. The flexibility of the ligand is given by dihedral angle variations. Various solutions evaluated by a score, are usually equivalent to the absolute value of the total energy of the ligand in the protein environment. Simulations were ranked according to the docked energy between the protein and the ligand, a summation of internal ligand energy and intermolecular energy terms.

3 RESULTS AND DISCUSSION

3.1 Homology Modeling of the rpoB Protein

A high level of sequence identity usually ensures accurate alignment between the target sequence and template structure. In the results of BLAST search against PDB, the–reference proteins, including crystal structure of *Thermus thermophilus* RNA polymerase holoenzyme at 3.3 Å resolution (PDB: 2CW0) [40], crystal structure of *T. thermophilus* RNA polymerase holoenzyme complexed with inhibitor tagetitoxin (PDB: 2BE5) [41], crystal structure of *T. thermophilus* RNA polymerase holoenzyme complexed with antibiotic streptolydigin (PDB: 2A6H) [42], crystal structure of *T. thermophilus* RNA polymerase holoenzyme (PDB: 2A6E) [43], crystal structure of *T. thermophilus* RNA polymerase holoenzyme complexed with antibiotic rifapentin (PDB: 2A69) [44], crystal structure of *T. thermophilus* RNA polymerase holoenzyme complexed with antibiotic rifabutin (PDB: 2A68) [45], structure of *T. thermophilus* RNA polymerase holoenzyme complexed with antibiotic streptolydigin (PDB: 1ZYR) [46], structural basis for transcription regulation by alarmone ppGpp (PDB: 1SMY) [47], and crystal structure of RNA polymerase holoenzyme from *T. thermophilus* at 2.6 Å resolution (PDB: 1IW7) [48], have a high level of sequence identity. The identity of these reference proteins with the rpoB was 50% (Table 1).

Table 1. Data for the closest homologue with known 3D structures obtained with the BLAST server against PDB

PDB	Protein	Chain	Authors	% identity to query
2CW0	Crystal structure of *Thermus thermophilus* RNA polymerase holoenzyme at 3.3 Å resolution	C,M	Tuske, *et al*. 2005	50
2BE5	Crystal structure of the *T. thermophilus* RNA polymerase holoenzyme in complex with Inhibitor tagetitoxin	C	Vassylyev *et al*. 2005	50
2A6H	Crystal structure of the *T. thermophilus* RNA polymerase holoenzyme in complex with antibiotic sterptolydigin	C,M	Temiakov *et al*. 2005	50
2A6E	Crystal structure of the *T. thermophilus* RNA polymerase holoenzyme	C,M	Artsimovitch *et al*. 2005	50
2A69	Crystal structure of the *T. thermophilus* RNA Po polymerase holoenzyme in complex with antibiotic rifapentin	C,M	Artsimovitch *et al*. 2005	50
2A68	Crystal structure of the *T. thermophilus* RNA polymerase holoenzyme in complex with antibiotic rifabutin	C,M	Artsimovitch., *et al*. 2005	50
1ZYR	Crystal structure of the *T. thermophilus* RNA polymerase holoenzyme in complex with antibiotic streptolydigin	C,M	Tuske 2005	50
1SMY	Structural basis for transcription regulation by alarmone ppgpp	C,M	Artsimovitch *et al*. 2005	50
1IW7	Crystal structure of the RNA polymerase holoenzyme from *T. thermophilus* at 2.6 Å resolution	C,M	Vassylyev *et al*. 2002	50

Table 2. Options used in the MODELLER program

SET ALNFILE	Alignment 1
SET KNOWNS	2CW0
SET SEQUENCE	Query
SET HETATM_IO	on
SET WATR_IO	off
SET HYDROGEN	off
SET STARTING_MODEL	1
SET ENDING_MODEL	20
CALL ROUTINE	Model

In the subsequent studies, the crystal structure of 2CW0 chain C was used as a template for modeling rpoB. The sequence identity between 2CW0 and rpoB is 50%, which makes 2CW0 a good template for modeling. Coordinates from the reference protein (2CW0) to the structurally conserved regions (SCRs), structurally variable regions (SVRs), N and C–termini were assigned to the target sequence based on the satisfaction of spatial restraints. All side chains of the modeled protein were set by rotamers. The structure was then minimized using conjugate gradient energy minimization and subjected to molecular dynamics using CHARMM force field. The options used for running the modeler are shown in Table 2. The final structure having least energy was then minimized with SYBYL software using Powell and conjugate energy minimization methods. The final energy of the minimized structure was –1832.696 kcal/mol and has RMS force value of 0.046 kcal/mol Å with a bond stretching energy of 444.4 kcal/mol, angle bending energy of 2419.9 kcal/mol, torsional energy of 2638.9 kcal/mol, out of plane bending energy of 47.528 kcal/mol, 1–4 van der Waals energy of 1372.9 kcal/mol, van der Walls energy of –8137.8 kcal/mol, 1–4 electrostatic energy of 1619.7 kcal/mol and electrostatic energy of –2238.4 kcal/mol. The initial model was thus generated with the above procedure. The final stable structure of the rpoB obtained is shown in Figure 1, which reveals that this protein has 28 α–helices, 42 β–sheets and 45 turns.

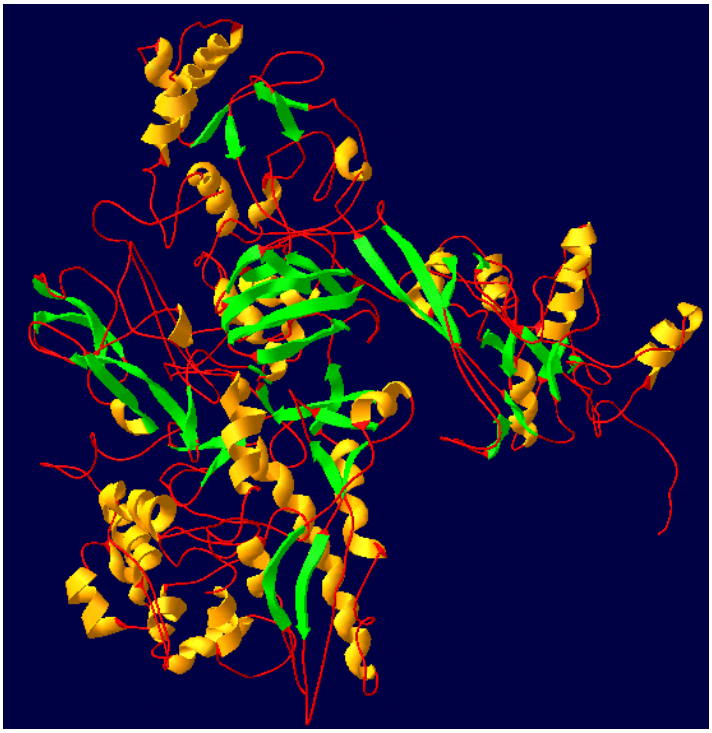

Figure 1. The final 3D structure of rpoB enzyme. The structure is obtained by energy minimizing with 100 steps of Powell and 10000 steps of conjugate gradient method until the convergence is reached. α–Helices are represented in orange and β–sheets in green color

Table 3. Ramachandran plot calculations on 3D model of rpoB computed with the PROCHECK program

% of residues in most favored regions	71.2
% of residues in the additionally allowed zones	26.7
% of residues in the generously regions	1.9
% of residues in disallowed regions	0.3
% of non–glycine and non–proline residues	100.0

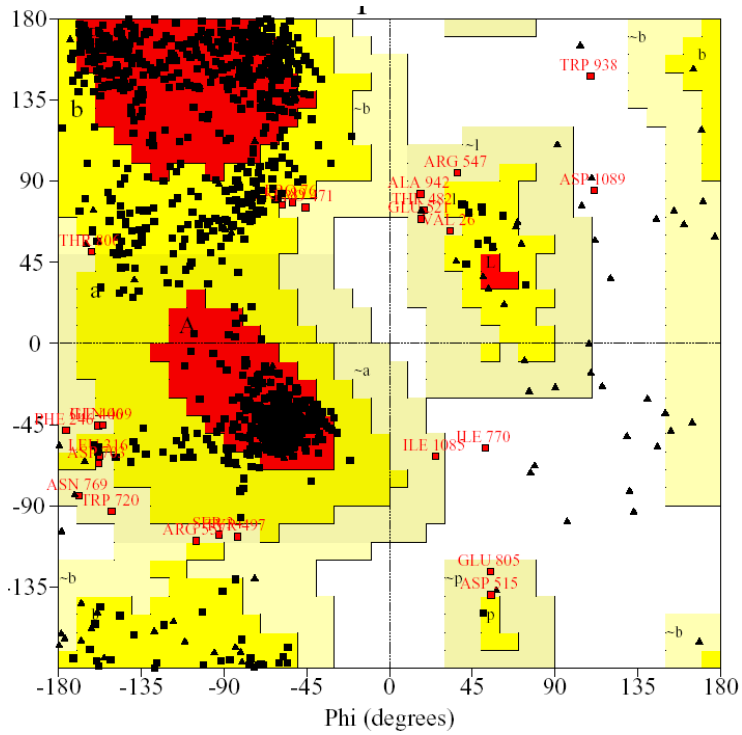

Figure 2. Ramachandran's map of rpoB enzyme. The plot calculations on 3D model of rpoB enzyme computed with the PROCHECK program

3.2 Validation of the rpob Model

Validation of the rpoB model was carried out using Ramachandran plot calculations computed with the PROCHECK program. The ϕ and φ distributions of the Ramachandran plot of non–glycine, non–proline residues are summarized in Figure 2 and Table 3. It appears from Figure 3 and Table 3 that 71% of the ϕ–φ angles are located in the core regions of the Ramachandran plot, 26.7% are in the additionally allowed zones, 1.7% of the residues in the generously allowed regions and 0.3% of the residues are in disallowed regions. This is very similar to the data from the template where 67% of the residues are in the favorable regions, 31.7% are in additionally allowed regions, 1.1% of the residues are in the generously allowed regions and 0.2% are in disallowed regions. This is an evidence to believe that the structure of rpoB built is reliable. The RMSD for covalent bonds relative to the standard dictionary was –0.26 Å and for the covalent angles was –0.52°. Altogether 99.7% of the residues was in favored and allowed regions. The overall PROCHECK G–factor was –0.39. The final structure was validated by ERRAT graph and the results are shown in Figure 3. The quality factor of 64.3 in the ERRAT graph (Figure 3) corresponded to an acceptable 3D profile. Further evaluation of the final model with Whatif program predicted the RMS Z scores of

backbone–backbone contacts (–1.99), backbone–side chain contacts (–2.60), side chain–backbone contacts (–2.64), side chain–side chain contacts (–1.93), and overall contacts Z score (–2.79). These values appeared lesser than the normal value of 2.0 and hence this final refined model is used for further analysis.

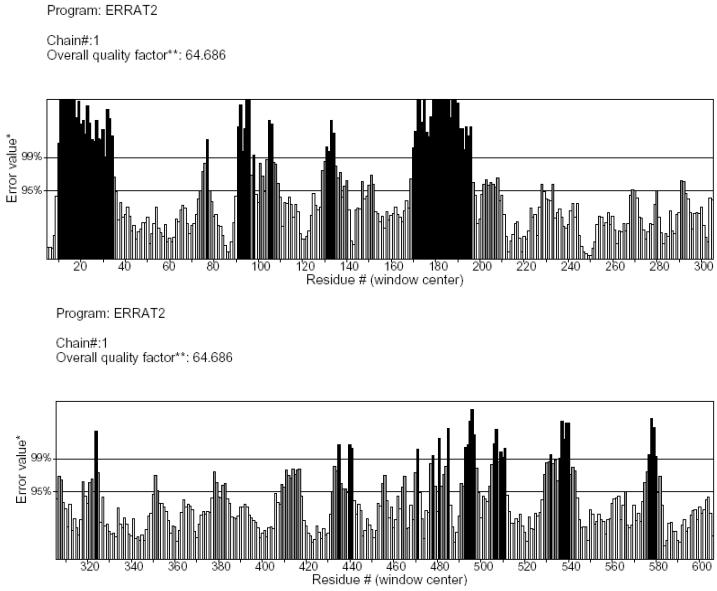

Figure 3. The 3D profiles verified results of rpoB model, residues with positive compatibility score are reasonably folded.

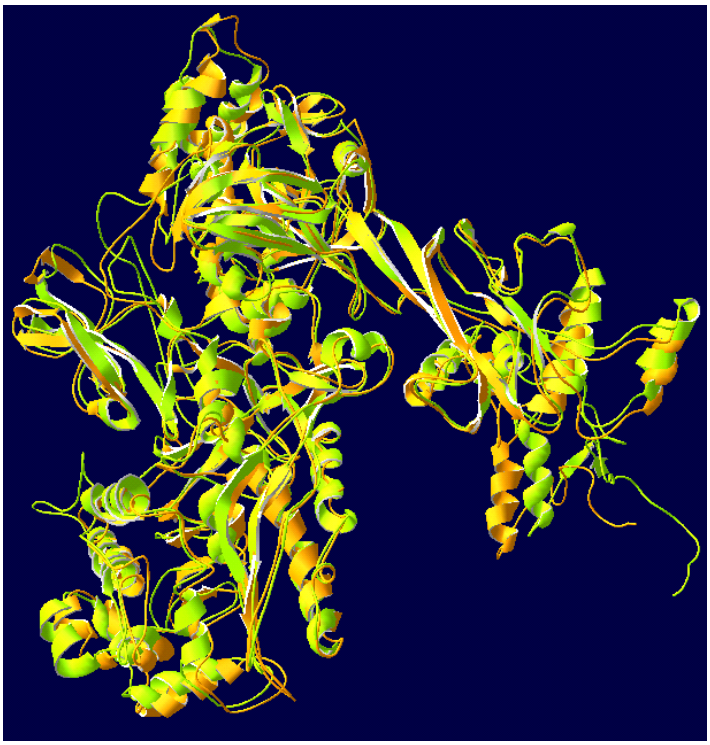

Figure 4. Superimposition of Cα trace of rpoB (green) and 2CW0 (orange).

3.3 Structural Superimposition of 2CW0 with rpoB

The structural superimposition of Cα trace of template and rpoB protein is shown in Figure 4. The weighted RMSD of Cα trace between initial and final refined models of rpoB predicted using SPDBV software are 0.04 Å, and the weighted RMSD of Cα trace between 2CW0 and rpoB was 1.5 Å. The RMSD of Cα trace between 2CW0 and rpoB calculated using the Superpose server [49] is shown in Table 4, and reveals that local RMSD of Cα trace between template and the model built was 0.95 Å and the local RMSD of backbone was 0.99 Å. This value indicates that the structure is highly reliable. Hence, this model was used for the identification of active site and for docking of the inhibitors with rpoB.

Table 4. Local and Global RMSD calculations of rpoB and 1CW0 using superpose server

	Alpha carbons	Back bone	Heavy	All
Local RMSD	0.95	0.99	1.64	1.64
Global RMSD	8.35	8.33	8.36	8.36

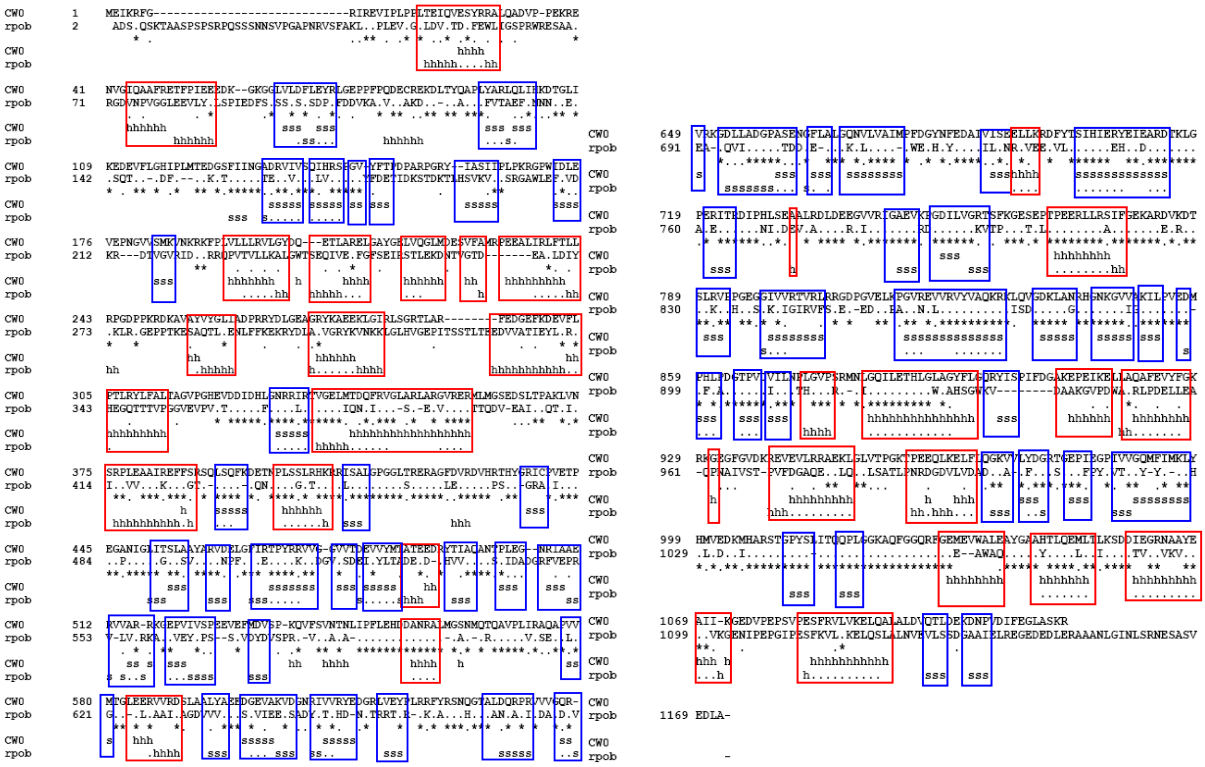

Figure 5. Structure–structure alignment of template, and the final structure of the rpoB enzyme using clustalW. Boxes colored with red indicate conserved α–helices and boxes colored with blue indicate conserved β–sheets.

3.4 Secondary Structure Prediction

Secondary structures of the model built were analyzed with the template by structure–structure comparison using SPDBV software suite (http://www.expasy.org/spdbv software) [50]. It was found that secondary structures of template and final rpoB are highly conserved with 28 α–helices, 45 β–sheets in the rpoB structure, 29 α–helices and 45 β–sheets with one extra α–helix in the

template (Figure 5). In spite of several amino acid differences in the primary structures of 2CW0 and the rpoB protein, their secondary structures were found identical and were further used for active site identification.

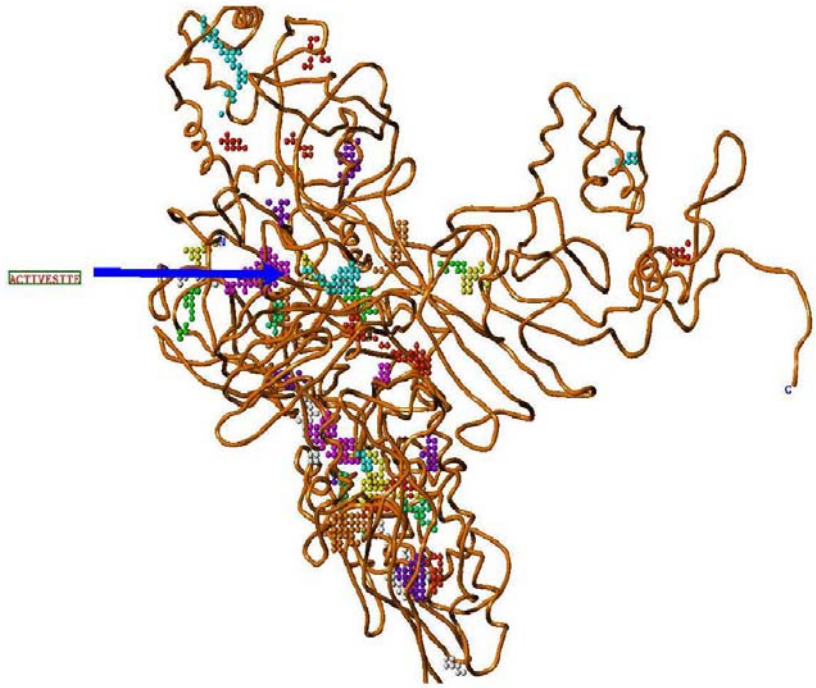

Figure 6. The possible binding–sites of rpoB model. The active site region is represented with an arrow.

3.5 Active Site Identification for the rpoB Protein

After the final model was built, the possible binding sites of rpoB were searched using the SiteID module of SYBYL software suite implemented on silicon graphics $O2^+$ working station and 12 possible binding sites were obtained (Figure 6). These pockets were compared with the active site of the template and were found that site 4 (violet region; Site 4) is highly conserved with the catalytic site of the template 2CW0.

Thus, in this study, site 4 is chosen as the more favorable binding site to dock the inhibitors, and hence the other eleven sites are not discussed further. The protein rpoB from *M. tuberculosis* and the 1CW0 from *T. thermophilu*s are well conserved in both sequence and structure; therefore, their biological function may be identical. In fact, from the structure–structure comparison of template, and final refined models of rpoB using SPDBV program, it was found that secondary structures are highly conserved. Also, the residues in the site4; Ala584, Thr585, Ala586, Pro611, Leu612, Thr829, Lys832, Pro834, Gly839, Gln961, Pro962, Thr968, and Val970 are highly conserved with the active site of template 2CW0 (Figure 5). It was found that the active site residues of the model generated using MODELLER6v2 software, Ala584 is interacting with Ser582, Met587, Glu606; Thr585 with

Ser582, Glu481, Ile581; Thr829 with Asp828; Lys832 with Ser830; Gly839 with Val790; Pro962 with Glu959; Val970 with Ser967.

These interactions were also calculated after simulations and found that Ala586 is interacting with Ser582; Thr829 with Lys799; Gly839 with Val790; Gln961 with Glu959; Thr968 with Asp972 and Val970 with Ser967 and Ala974. These interactions before and after simulations are involved in conformational changes in the active site of the protein and are responsible for binding of the inhibitors with high efficacy. The RMSD of Cα trace between 2CW0 and rpoB active sites was also calculated using SPDBV software suite and found to be 0.79Å, predicting that the structure is reliable. This suggested that inhibitors bind in a similar manner for both rpoB and 2CW0. The active site residues Ala584, Thr585, Ala586, Pro611, Lue612, Thr829, Lys832, Pro834, Gly839, Gln961, Pro962, Thr968, and Val970 are conserved in these two enzymes and may be important for structural integrity or maintaining the hydrophobicity of the inhibitor binding pocket. These residues showed similarity with Asn543, Thr544, Asn546, Pro570, Leu571, Thr788, Arg791, Pro793, Gly798, Lys930, Gly931, Asp937 and Glu940 of the template active site. In these active sites, Asn543, Asn545, Arg791, Lys930, Gly931, Asp937, and Glu940 substituted residues Ala584, Ala586, Lys832, Gly961, Pro962, Thr968, and Val970.

It appears that substitution of Ser425 with Leu464 was also responsible for rifampin resistance in rpoB. It was found that Val570, Ser567, and Arg556 replaced the residues Phe531, Pro526 and Arg516 in the template in the rpoB protein. Therefore, these residues in the active site may be responsible for rifampin resistance. Studies have shown that mutations are located in a short, evolutionarily well conserved, cluster I of region II that is known as the site of mutations that confer resistance in *E. coli* [51]. It appears that drug resistance in *M. leprae* is caused by the mutation of Ser425 to Phe that is present in cluster I of *M. leprae* and *E. coli*. Substitution of Ser425 by bulkier, hydrophobic groups of Met, Leu and Phe would result in a physical obstruction for rifampin as it diffuses into a functionally important crevice with in the enzyme. Nearly 82% of the isolates from *M. tuberculosis* contain missense mutations, leading to substitution of amino acids at Ser531 (41.9%), His526 (32.9%) and Asp516 (7.3%) residues. Other missense mutations, as well as insertion and deletion mutations, were also observed in *M. tuberculosis* strains leading to rifampicin resistance.

Similar mutations and frequencies of codon substitution in Rif^r *M. tuberculosis* isolates were reported previously [52–54]. Besides, six mutations were observed in rpoB resistant gene in *M. tuberculosis* at Met521, Thr509, Leu526, Gln527, Gly516, and Pro513. In *E. coli*, it was shown that Pro513 substituted amino acid was associated with high level of resistance [55]. It was also found

that mutations in Leu526 and Gly516 amino acids lead to high–level resistance to the drug in both *E.coli* and *M.Tuberculosis*. It was observed that many of the mutant alleles of *E. coli* encode β–subunits, which display pleotrophic conditional defects in addition to rifampin resistance [50,55].

Table 5. List of compounds used for docking in this study

Compound	Compound	Compound
2–Aminobutanic acid	Ethambutal	PAS (p–aminosalicylic acid)
4–Aminobutanic acid	Ethionamide	Pyrazinamide
Ciprofloxacin	Glycine	Rifampicin
Clofazimine	Isoniazid	Rifampin
Cycloserine	Kanamycin	Streptomycin
2–Alanylaminopropanoic acid	Oflaxacin	Thioacetazone

Table 6. Total (E_{total}), electrostatic (E_{ele}), steric energies (E_{ste}) of the best–docked conformations

Molecule	Total energy kcal/mol	Steric energy kcal/mol	Electrostatic energy kcal/mol
2–aminobutanic acid	42.6	60.6	–17.9
4–aminobutanic acid	309.7	317.4	–7.7
Ciprofloxain	–3.5	2.9	–6.4
Kanamycin	832.3	899.7	–67.3
Oflaxacin	411.8	409.3	2.5
Pyrizinamide	13.9	18.9	–4.9

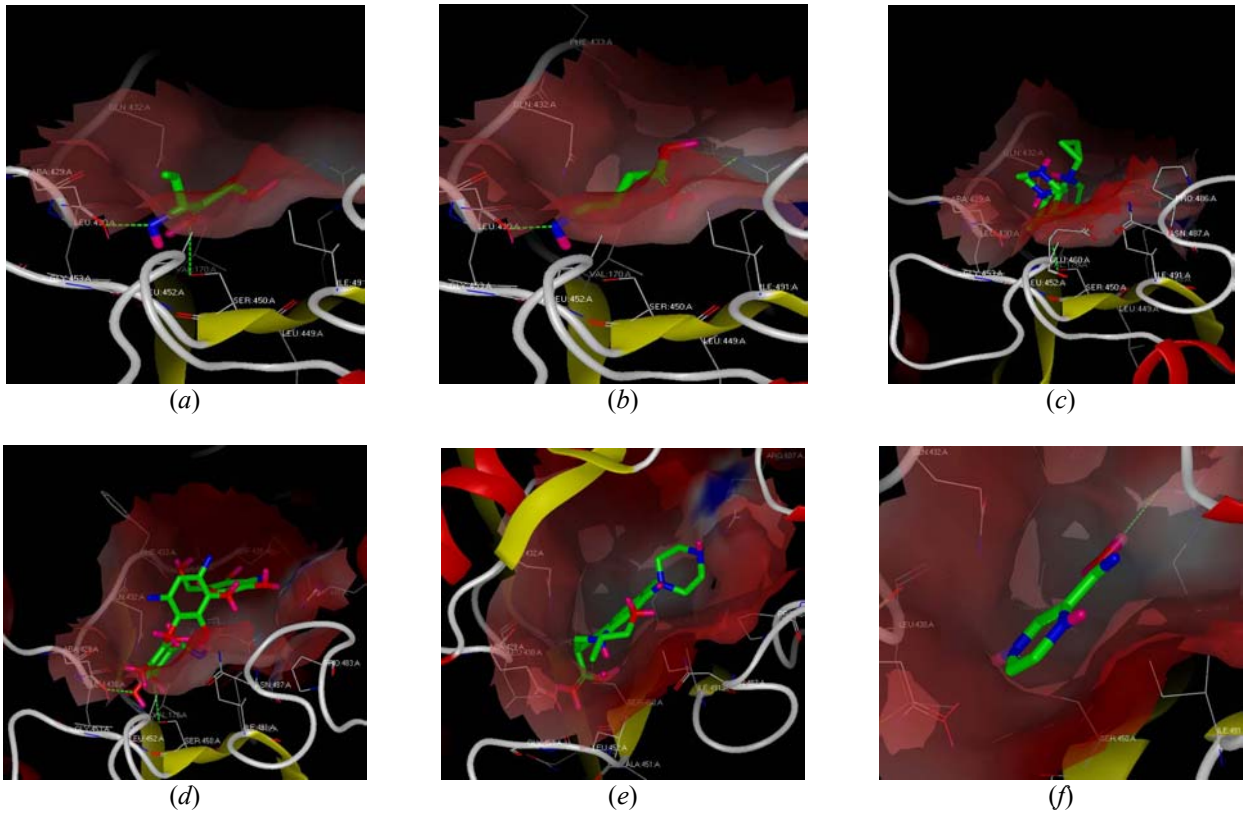

Figure 7. Binding of inhibitors to rpoB enzyme. Inhibitors are represented in green color. (*a*) rpoB and 2–aminobutanic acid complex; (*b*) rpoB and 4–aminobutanicacid; (*c*) rpoB and ciproflaxacin; (*d*) rpoB and kanamycin; (*e*) rpoB and oflaxacin; (*f*) rpoB and pyrizanamide.

3.6 Docking of Inhibitors in the Active Site of rpoB

All 18 compounds listed in Table 5 were used for docking with rpoB using GOLD for 50 cycles. By automated docking, the top ranking protein–ligand conformations were analyzed for each inhibitor. To understand the interaction between rpoB enzyme and inhibitors, the rpoB–inhibitor complex was generated using the SYBYL software suite (Figure 7). The binding interactions were characterized by the ligand binding energies against the rpoB model using the DOCK module of the SYBYL software. It was found that 2–aminobutanic, 4–aminobutanic, ciprofloxain, kanamycin, oflaxacin, and pyrizinamide have 42.6, 309.7, –3.5, 823.3, 411.8 and 13.9 kcal/mol of energy respectively. Table 6 shows the interaction energies including the total, electrostatic and steric for all the residues in the active site of enzyme–inhibitor complex. Based on these studies, it was found that enzyme–ciprofloxain inhibitor complex exhibited a favorable total interaction energy of –3.518 kcal/mol. The electrostatic and steric energies were found as –6.460 and 2.942 kcal/mol respectively. These results revealed that ciprofloxacin is the best inhibitor for rpoB protein compared with the other inhibitors used in this study. The hydrogen bonds present in enzyme–inhibitor complex along with their distances and angles are listed in Table 7.

Table 7. Hydrogen bonds along with their distances and angles between the substrate, inhibitors and active site residues of rpoB as deciphered using SYBLY software suite

Molecule	H–Bonds Amino acid ligand atom	Distance (Å)	Angle (°)
2–Aminobutanic acid	Arg448H……..O1	2.5	115
	Gln4290E1……...H5	1.9	123
4–Aminobutanic acid	Arg448H…….O_1	2.1	77
	Arg448H……..O_2	2.2	150
	Ser450H9…….N_1	2.2	98
	Gln4290E1……H_8	1.9	168
Ciprofloxain	Arg448H……...O_1	2.0	113
	Ser450Hg……O_2	2.0	148
Kanamycin	Arg448.HH12…O3	2.6	127
	Arg448H…….N4	1.9	120
	Ser450H9……...O8	2.0	105
	Gln4290E1……. H15	2.0	176
Oflaxacin	Ser450HG……O4	2.0	110
Pyrizinamide	Arg448H……..O1	2.0	118
	Ser450HG…….N	1.7	86

It was found from the Table 7 that 2–aminobutanic, 4–aminobutanic, ciprofloxain, kanamycin, oflaxacin, and pyrizinamide have two, four, two, four, one and two hydrogen bonding interactions respectively. It is also evident from the Figure 7 that inhibitors are located in the center of the active site, and are stabilized by hydrogen bonding interactions. Key residues in the active site of the model were determined based on hydrogen bonding interactions of the inhibitors with residues in the active site of rpoB. This identification reveals the relative significance for every residue. Through the interaction analysis, it is noticed that Gln429, Arg448 and Ser450 are important

anchoring residues for the inhibitors and are the main contributors to the inhibitor interactions. Though the interaction energy does not include the contribution from the water or the extended protein structure, this preliminary data along with the list of hydrogen bond interactions between the enzyme and the active site residues clearly support that Gln429, Arg448 and Ser450 are more preferred residues in the binding of inhibitors. The interaction between the enzyme and the inhibitors proposed in this study are useful for understanding the potential mechanism of enzyme and the binding of inhibitors. As is well known, hydrogen bonds play an important role for the structure and function of biological molecules, especially for the rpoB catalysis. It was found that while inhibitors 2– and 4–aminobutanic acids are binding with Arg448 and Gln 429; Arg448, Ser450, and Gln 429 respectively, ciprofloxacin is binding with Arg448 and Ser450; kanamycin with Arg448, Ser450 and Gln429; ofloxacin with Ser450 and pyrizanamide with Arg448, and Ser450. These studies show that Gln429, Arg448 and Ser450 are important for strong hydrogen bonding interactions with the inhibitors. Furthermore, Gln429, Arg448 and Ser450 residues are involved in inhibitor binding and are conserved between these two enzymes (2CW0 and rpoB) and form hydrogen bonding with the inhibitors. To the best of our knowledge Gln429, Arg448 and Ser450 are important determinant residues in inhibitor binding and are responsible for rifampin resistance in *M. leprae*.

4 CONCLUSIONS

Rifampin is currently the most potent drug used in leprosy control programs. Rifampin resistance was due to mutations in the β subunit of RNA polymerase of Mycobacterium leprae encoded by *rpoB* gene. Inhibition of the rpoB protein reduces lepromatous leprosy. To predict the role of rpoB protein a three-dimensional structure of rpoB was predicted using the software MODELLER6v2 and further minimized using SYBYL software. Validation of the protein was done by the programs PROCHECK and errat which show that the protein is reliable. Molecular docking was carried out for a set of known molecules with the built model using Fast Exhaustive Rigid body Docking (FRED). Results show that ciproflaxin is the best inhibitor against rifampin resistant rpoB protein. The detailed analysis of the resulted rpoB ligand complexes may improve our knowledge in understanding the binding interactions. Thus, this study offers a route to the discovery of new drugs against rifamipin resistance rpoB protein.

Acknowledgment

The authors are thankful to the Director, Center for Distance Education, Osmania University, Hyderabad for his support, cooperation and for providing facilities to carry out this work.

5 REFERENCES

[1] L. B. Heifets and G. A. Cangelosi. Drug susceptibility testing of *Mycobacterium tuberculosis*: a neglected problem at the turn of the century. Int. *J. Tuberc. Lung Dis.* **1999**, *3*, 564–581.

[2] C. Dye, S. Scheele, P. Dolin, V. Pathania, and M. C. Raviglione. Consensus statement. Global burden of tuberculosis: estimated incidence, prevalence, and mortality by country. WHO Global Surveillance and Monitoring Project. *JAMA* **1999**, *282*, 677–686.

[3] T. R. Gingeras, G. Ghandour, E. Wang, A. Berno, P. M. Small, F. Drobniewski, D. Alland, E. Desmond, M. Holodniy, and J. Drenkow. Simultaneous genotyping and species identification using hybridization pattern recognition analysis of generic *Mycobacterium* DNA arrays. *Genome Res.* **1998**, *8*, 435–448.

[4] S. V. Hetherington, A. S. Watson, and C. C. Patrick. Sequence and analysis of the *rpoB* gene of *Mycobacterium smegmatis*. *Antimicrob. Agents Chemother.* **1995**, *39*, 2164–2166.

[5] N. T. Honore, S. Bergh, S. Chanteau, F. Doucet–Populaire, K. Eiglmeier, T. Garnier, C. Georges, P. Launois, T. Limpaiboon, S. Newton, K. Niang, P. Del Portillo, G. R. Ramesh, P. Reddi, P. R. Ridel, N. Sittisombut, S. Wu–Hunter, and S. T. Cole. Nucleotide sequence of the first cosmid from the *Mycobacterium leprae* genome project: structure and function of the Rif–Str regions. *Mol. Microbiol.* **1993**, *7*, 207–214.

[6] L. P. Miller, J. T. Crawford, and T. M. Shinnick. The *rpoB* gene of *Mycobacterium tuberculosis*. *Antimicrob. Agents Chemother.* **1994**, *38*, 805–811.

[7] A. Telenti, P. Imboden, F. Marchesi, D. Lowrie, S. Cole, M. J. Colston, L. Matter, K. Schopfer, and T. Bodmer. Detection of rifampin–resistance mutations in *Mycobacterium tuberculosis*. *Lancet* **1993**, *341*, 647–650.

[8] J. H. Grosset and B. Ji. Recent advances in the chemotherapy of leprosy. *Lepr. Rev.* **1990**, *61*, 313–329.

[9] World Health Organization, Special Working Group. **1982**. Chemotherapy of leprosy for control programmes. Technical Report Series 675. World Health Organization, Geneva.

[10] T. R. Frieden, T. Sterling, A. Pablos–Mendez, J. O. Kilburn, G. M. Cauthen, and S. W. Dooley. The emergence of drug–resistant tuberculosis in New York City. *N. Engl. J. Med.* **1993**, *328*, 521–526.

[11] M. Goble, M. D. Iseman, L. A. Madsen, D. Waite, L. Ackerson, and C. R. Horsburgh. Treatment of 171 patients with pulmonary tuberculosis resistant to isoniazid and rifampin. *N. Engl. J. Med.* **1993**, *328*, 527–532.

[12] J. H. Grosset, C. C. Guelpa–Lauras, P. Bobin, G. Brucker, J. L. Cartel, M. Constant–Desportes, B. Flageul, M. Frederic, J. C. Guillaume, and J. Millan. Study of 39 documented relapses of multibacillary leprosy after treatment with rifampin. *Int. J. Lepr.* **1990**, *57*, 607–614.

[13] N. Honore and S. T. Cole. Molecular basis of rifampin resistance in *Mycobacterium leprae*. *Antimicrob. Agents Chemother.* **1993**, *37*, 414–418.

[14] P. Steiner, M. Rao, M. Mitchell, and M. Steiner. Primary drug–resistant strains of *M. tuberculosis* to rifampin. *Ann. Rev. Respir. Dis.* **1986**, *134*, 446–448.

[15] K. D. Stottmeir, Emergence of rifampin–resistant *Mycobacterium tuberculosis* in Massachusetts. *J. Infect. Dis.* **1976**, *133*, 88–90.

[16] L. Levy, Studies of the mouse footpad technique for cultivation of *Mycobacterium leprae*. III. Doubling time during logarithmic multiplication. *Lepr. Rev.* **1976**, *47*, 103–106.

[17] Y. A. Ovchinnikov, G. S. Monastyrskaya, V. V. Gubanov, V. M. Lipkin, E. D. Sverdlov, I. F. Kiver, I. A. Bass, S. Z. Mindlin, 0. N. Danilevskaya, and R. B. Khesin. Primary structure of *Escherichia coli* RNA polymerase. Nucleotide substitution in the beta subunit gene of the rifampicin resistant *rpoB*255 mutant. *Mol. Gen. Genet.* **1981**, *184*, 536–538.

[18] Y. A. Ovchinnikov, G. S. Monastyrskaya, S. O. Guriev, N. F. Kalinina, E. D. Sverdlov, A. I. Gragerov, I. A. Bass, I. F. Kiver, E. P. Moiseyeva, V. N. Igumnov, S. Z. Mindlin, V. G. Nikiforov, and R. B. Khesin. RNA polymerase rifampicin resistance mutations in *Escherichia coli*: sequence changes and dominance. *Mol. Gen. Genet.* **1983**, *190*, 344–348.

[19] G. M. Yepiz–Plascencia, C. A. Radebaugh, and R. B. Hallick. The *Euglena gracilis* chloroplast *rpoB* gene. Novel gene organization and transcription of the RNA polymerase subunit operon. *Nucleic Acids Res.* **1990**, *18*, 1869–1878.

[20] L. A. Allison, M. Moyle, M. Shales, and C. J. Ingles. Extensive homology among the largest subunits of eukaryotic and prokaryotic RNA polymerases. *Cell* **1985**, *42*, 599–610.

[21] D. Falkenburg, B. Dworniczak, D. M. Faust, and E. K. F. Bautz. RNA polymerase II of *Drosophila*: relation of its 140,000 Mr subunit to the β subunit of *Escherichia coli* RNA polymerase. *J. Mol. Biol.* **1987**, *195*, 929–937.

[22] D. Sweetser, M. Nonet, and R. A. Young. Prokaryotic and eukaryotic RNA polymerases have homologous core subunits. *Proc. Natl. Acad. Sci. USA* **1987**, *84*, 1192–1196.

[23] N. A. Woychik and R. A. Young. RNA polymerase II: subunit structure and function. *Trends Biochem. Sci.* **1990**, *15*, 347–351.

[24] D. J. Jin and C. A. Gross. Mapping and sequencing of mutations in the *Escherichia coli rpoB* gene that lead to rifampin resistance. *J. Mol. Biol.* **1988**, *202*, 45–58.
[25] N. A. Lisitsyn, E. D. Sverdlov, E. P. Moiseyeva, O. N. Danilevskaya, and V. G. Nildforov. Mutation to rifampin resistance at the beginning of the RNA polymerase beta subunit gene in *Eschenchia coli*. *Mol. Gen. Genet.* **1984**, *196*, 173–174.
[26] Y. A. Ovchinnikov, G. S. Monastyrskaya, V. V. Gubanov, V. M. Lipkin, E. D. Sverdlov, I. F. Kiver, I. A. Bass, S. Z. Mindlin, O. N. Danilevskaya, and R. B. Khesin. Primary structure of *Escherichia coli* RNA polymerase. Nucleotide substitution in the beta subunit gene of the rifampicin resistant *rpoB*255 mutant. *Mol. Gen. Genet.* **1981**, *184*, 536–538.
[27] Y. A. Ovchinnikov, G. S. Monastyrskaya, S. O. Guriev, N. F. Kalinina, E. D. Sverdlov, A. I. Gragerov, I. A. Bass, I. F. Kiver, E. P. Moiseyeva, V. N. Igumnov, S. Z. Mindlin, V. G. Nikiforov, and R. B. Khesin. RNA polymerase rifampicin resistance mutations in *Escherichia coli*: sequence changes and dominance. *Mol. Gen. Genet.* **1983**, *190*, 344–348.
[28] N. Honore, S. Bergh, S. Chanteau, F. Doucet–Populaire, K. Eigimeier, T. Garnier, C. Georges, P. Launois, P. Limpaiboon, S. Newton, K. Nyang, P. del Portillo, G. K. Ramesh, T. Reddy, J. P. Riedel, N. Sittisombut, S. Wu–Hunter, and S. T. Cole. Nucleotide sequence of the first cosmid from the *Mycobacterium leprae* genome project: structure and function of the Rif–Str regions. *Mol. Microbiol.* **1992**, *7*, 207–214.
[29] S. F. Altschul, W. Gish, W. Miller, E. W. Myers, and D. J. Lipman, Basic local alignment search tool. *J. Mol. Biol.* **1990**, *215*, 403–410.
[30] S. F. Altschul, T. L. Madden, A. A. Schaffer, J. Zhang, Z. Zhang, W. Miller, and D. J. Lipman, Gapped BLAST and PSI–BLAST: a new generation of protein database search programs. *Nucleic Acids Res.* **1997**, *50*, 3389–3402.
[31] A. Sali and T. L. Blundell, Comparative protein modeling by satisfaction of spatial restraints. *J. Mol. Biol.* **1993**, *234*, 779–815.
[32] J. D. Thompson, D. G. Higgins, and T. J. Gibson, CLUSTAL W: improving the sensitivity of progressive multiple sequence alignment through sequence weighting, position–specific gap penalties and weight matrix choice. *Nucleic Acids Res.* **1994**, *22*, 4673–4680.
[33] S. B. Needleman and C. D. Wunsch, A general method applicable to the search for similarities in the amino acid sequence of two proteins. *J. Mol. Biol.* **1970**, *48*, 443–453.
[34] N. Guex and M. C. Peitsch. SWISS–MODEL and the Swiss–PdbViewer: an environment for comparative protein modelling. *Electrophoresis* **1997**, *18*, 2714–2723.
[35] R. A. Laskoswki, M. W. MacArthur, D. S. Moss, and J. M. Thornton, PROCHECK: a program to check the stereo chemical quality of protein structures. *J. Appl. Cryst.* 1993, *26*, 283–291.
[36] K. Colovos and T. O. Yeates, Verification of protein structures: Patterns of nonbonded atomic interactions. *Protein Sci.* **1993**, *2*, 1511–1519.
[37] G. Vriend et al., WHAT IF: a molecular modeling and drug design program, *J. Mol. Graph.* **1990**, 8, 52–56.
[38] C. M. Ho and G. R. Marshall, Cavity search: an algorithm for isolation and display of cavity–like binding regions. *J. Comput.–Aided Mol. Des.* **1990**, *4*, 337–354.
[39] G. Jones, P. Willett, R. C. Glen, A. R. Leach, and R. Taylor, Development and validation of a genetic algorithm for flexible docking. *J. Mol. Biol.* **1997**, *267*, 727–748.
[40] I. Artsimovitch, M. N. Vassylyeva, D. Svetlov, V. Svetlov, A. Perederina, N. Igarashi, N. Matsugaki, S. Wakatsuki, T. H. Tahirov, and D. G. Vassylyev, Allosteric modulation of the RNA polymerase catalytic reaction is an essential component of transcription control by rifamycins. *Cell* **2005**, *122*, 351–363.
[41] I. Artsimovitch, V. Patlan, S. Sekine, M. N. Vassylyeva, T. Hosaka, K. Ochi, S. Yokoyama, and D. G. Vassylyev, Structural basis for transcription regulation by alarmone ppGpp *Cell* **2004**, *117*, 299–310.
[42] S. Tuske, S. G. Sarafianos, X. Wang, B. Hudson, E. Sineva, J. Mukhopadhyay, J. J. Birktoft, O. Leroy, S. Ismail, A. D. Clark, Jr, C. Dharia, A. Napoli, O. Laptenko, J. Lee, S. Borukhov, R. H. Ebright, and E. Arnold, Direct Submission to NCBI (Submitted (15–JUN–**2005**).
[43] D. Temiakov, N. Zenkin, M. N. Vassylyeva, A. Perederina, T. H. Tahirov, M. Savkina, S. Zorov, V. Nikiforov, N. Igarashi, N. Matsugaki, S. Wakatsuki, K. Severinov, and D. G. Vassylyev, Direct Submission, Submitted (02–JUL–**2005**).
[44] S. Tuske, S. G. Sarafianos, X. Wang, B. Hudson, E. Sineva, J. Mukhopadhyay, J. J. Birktoft, O. Leroy, S. Ismail, A. D. Clark, C. Dharia, A. Napoli, O. Laptenko, J. Lee, S. Borukhov, R. H. Ebright, and E. Arnold, Inhibition of bacterial RNA polymerase by streptolydigin: stabilization of a straight–bridge–helix active–center conformation. *Cell* **2005**, *122*, 541–552.
[45] D. G. Vassylyev, S. Sekine, O. Laptenko, J. Lee, M. N. Vassylyeva, S. Borukhov, and S. Yokoyama, Crystal structure of a bacterial RNA polymerase holoenzyme at 2.6 Å resolution. *Nature* **2002**, *417*, 712–719.
[46] D. G. Vassylyev, V. Svetlov, M. N. Vassylyeva, A. Perederina, N. Igarashi, N. Matsugaki, S. Wakatsuki, and I. Artsimovitch, Structural basis for transcription inhibition by tagetitoxin *Nature Struct. Mol. Biol.* **2005**, *12*, 1086–1093.

[47] D. G. Vassylyev, S. Sekine, O. Laptenko, J. Lee, M. N. Vassylyeva, S. Borukhov, and S. Yokoyama, Crystal structure of a bacterial RNA polymerase holoenzyme at 2.6 Å resolution *Nature* **2002**, *417*, 712–719.
[48] R. Maiti, G. H. Van Domselaar, H. Zhang, and D. S. Wishart, Superpose: a simple server for sophisticated structural superposition, *Nucleic Acids Res*. **2004**, *32*, W590–W594.
[49] N. Guex and M. C. Peitsch, SWISS–MODEL and the Swiss–Pdb Viewer: an environment for comparative protein modeling. *Electrophoresis* **1997**, *18*, 2714–2723.
[50] D. J. Jin and C. A. Gross. Mapping and sequencing of mutations in the Escherichia coli *rpoB* gene that lead to rifampicin resistance. *J. Mol. Biol*. **1988**, *202*, 45–58.
[51] V. Kapur, L. L. Li, S. Iordanescu, M. R. Hamrick, A. Wanger, B. N. Kreiswirth, and J. M. Musser. Characterization by automated DNA sequencing of mutations in the gene (*rpoB*) encoding the RNA polymerase B subunit in rifampin–resistant Mycobacterium tuberculosis strains from New York City and Texas. *J. Clin. Microbiol*. **1994**, *32*, 1095–1098.
[52] A. Telenti, P. Imboden, F. Marchesi, D. Lowrie, S. T. Cole, M. J. Colston, L. Matter, K. Schoolfer, and T. Bodmer. Detection of rifampicin–resistant mutations in Mycobacterium tuberculosis. *Lancet*.**1993**, *341*,647–650.
[53] A. Telenti, P. Imboden, F. Marchesi, T. Schmedheint, and T. Bodmer. Direct, automatic detection of rifampin–resistant Mycobacterium tuberculosis by polymerase chain reaction and single–strand conformation polymorphism analysis. *Antimicrob. Agents Chemother*. **1993**, *37*, 2054–2058.
[54] D. J. Jin and C. A. Gross. Mapping and sequencing of mutations in the Escherichia coli *rpoB* gene that lead to rifampicin resistance. *J. Mol. Biol*. **1988**, *202*, 45–58.
[55] D. J. Jin and C. A. Gross. Characterization of the pleiotropic phenotypes of rifampin–resistant *rpoB* mutants of Escherichia coli. *J. Bacteriol*. **1989**, *171*, 5229–5231.

Biographies

P. Nataraj Sekhar is a research scholar in the Department of Genetics. He is working with Dr. Ananda Reddy for his Ph.D. degree. Prof. P. B. Kavi Kishor is a professor in the Department of Genetics, Osmania University and is a co–guide to Mr. P. Nataraj Sekhar. Mr. V. C. K. Reddy is a Ph.D. student at the Osmania Medical College, Hyderabad. He also did his diploma from the Osmania University. Mr. E. Prem Kumar, A. Anitha and Mr. M. Ranjit Kumar, are postgraduate diploma students in bioinformatics of Osmania University and worked on this project as part of their diploma curriculum in the Genetics department.